Progress In Electromagnetics Research B, Vol. 109, 81-93, 2024

PIER B

(Received 25 September 2024, Accepted 26 November 2024, Scheduled 5 December 2024)

Design of a Crescent Moon-Shaped Reconfigurable Patch Antenna Using a PIN Diode for 5G Sub-6 GHz and Multistandard Wireless Applications

Salah E. El Aoud[1], Hind Abbaoui[2], Omaima Benkhadda[3], Sanae Attioui[1], Nasima El Assri[1], Saida Ibnyaich[1], Abdelouhab Zeroual[1], Mohd M. Ismail[4,*], and Ahmed J. A. Al-Gburi[4,*]

[1]*Laboratory of Instrumentation, Signals and Physical Systems (I2SP) Department of Physics, Faculty of Sciences Semlalia Cadi Ayyad University, Marrakesh, Morocco*
[2]*Laboratory of Electrical Systems, Energy Efficiency and Telecommunications (LSEEET) Department of Physics Faculty of Sciences and Techniques Gueliz, Cadi Ayyad University, Marrakesh, Morocco*
[3]*Laboratory of Mathematics, Computer Science, Electrical Engineering and Physics (LAMIGEP) Moroccan School of Engineering Sciences, Marrakesh, Morocco*
[4]*Faculty of Technology and Engineering Electronics and Computer, Universiti Teknikal Malaysia Melaka, Malaysia*

ABSTRACT: This research explores the versatility of a miniature reconfigurable antenna designed for a variety of wireless applications: 5G (IEEE 802.15.3), WLAN (IEEE 802.11), V2X (IEEE 802.11 p), WiMAX (IEEE 802.166), Wi-Fi 6E (IEEE 802.11 ax), Wi-Fi 7 (IEEE 802.11 be), C-band (from 4 GHz to 8 GHz), and X-band (from 8 GHz to 12 GHz). To enable frequency reconfigurability, the patch is equipped with two PIN diodes, which can be positioned at different locations to adjust the antenna's operational frequency range. This reconfigurability allows the antenna to maintain its size while changing its frequency range according to the state of the PIN diodes. The strength of our work lies in achieving exceptional electrical performance while maintaining a small size, cost-effective, and compact design. The antenna demonstrates an almost omnidirectional radiation pattern across all frequency ranges. Additionally, the simulated reflection coefficient remains within the ideal range for every frequency band. The antenna's overall dimension is $22 \times 18 \times 1.6\,\text{mm}^3$ ($\frac{\lambda_o}{4} \times \frac{\lambda_o}{5} \times \frac{\lambda_o}{56}$) (with λ_o being the free space wavelength at the lowest resonating frequency and for the proposed antenna its value equal to 91.18 mm) with a miniaturization rate equal to 75.25%. This compact antenna is designed to operate across multiple frequencies, making it suitable for various applications, particularly in wireless communication systems. Its versatility also makes it a promising candidate for future portable devices, sensor networks, and telecommunication applications. The performance metrics, including return loss and radiation pattern, are presented, demonstrating strong performance across these parameters. The analyses were conducted using the CST Studio Suite, which provided detailed insights into the antenna's functionality and effectiveness.

1. INTRODUCTION

Recently, there has been a significant increase in the demand for frequency-reconfigurable antennas, especially within the field of wireless communication [1, 2]. These antennas offer the capability to dynamically adjust various parameters, including radiation pattern, bandwidth, gain, and polarization, which enhances their adaptability to different communication needs [3–6]. Reconfigurability is typically achieved through the use of RF PIN diodes, varactor diodes, and Radio Frequency Microelectromechanical System (RF MEMS) switches [7, 8].

One of the most compelling advantages of reconfigurable antennas is their compact size, which makes them suitable for integration into space-constrained environments. Additionally, these antennas provide a consistent radiation pattern across all operational frequency bands, ensuring reliable performance [9, 10]. They also help to reduce co-site interference and jamming effects, contributing to improved signal clarity and system efficiency. These benefits make reconfigurable antennas a valuable asset in advancing modern wireless communication technologies [11, 12].

With the proliferation of diverse standards in cell phones and other personal mobile devices, there is a growing need for compact multi-band and smart antennas with reconfigurable features [13]. Ideally, a single antenna should support multiple functions, operating efficiently at different frequencies [14]. This versatility is crucial in managing the increased potential for interference among users sharing the same spectrum. As a result, antennas with the capability to dynamically place nulls are becoming increasingly important [15].

Reconfigurable antennas, both planar and three-dimensional (3-D), have been developed for a range of applications, including radar and wireless devices. For instance, various designs have been proposed for radar applications and wireless devices [16, 17]. Additionally, reconfigurable patch antennas specifically designed to operate in the L and X bands have also been introduced. These antennas offer enhanced flexibility and performance across different frequency ranges, addressing the evolving demands of modern communication systems [18, 19].

* Corresponding authors: Mohd M. Ismail (muzafar@utem.edu.my) and Ahmed J. A. Al-Gburi (ahmedjamal@ieee.org).

The 5G spectrum is divided into three primary bands: sub-1 GHz, sub-6 GHz, and millimeter-wave band [20]. Each of these primary bands is further segmented into multiple smaller bands, which are designated with specific numbers by the 3rd Generation Partnership Project (3GPP) in the Release 15 work items summary [21]. This detailed categorization helps to manage and allocate the frequency spectrum efficiently, ensuring that different applications and services within the 5G framework can operate effectively across various frequency ranges.

A variety of frequency-reconfigurable antenna structures are outlined in the literature. A compact, electronically tunable and single fed resonant slot antenna for higher frequency application has been reported. Many differential antennas operating at a single frequency or multi-frequency have been reported [22–27]. In [28], the authors propose the use of a single PIN diode to facilitate frequency reconfigurability, enabling a miniaturized flexible antenna to operate at three distinct frequencies.

In Multiple-Input Multiple-Output (MIMO) systems, a reconfigurable antenna array featuring two printed dipoles and PIN diode switches has been explored in [29]. This setup aims to enhance the system's versatility by allowing dynamic adjustments to both the radiation pattern and operating frequency. Similarly, annular slot antennas equipped with PIN diodes are designed to achieve reconfigurability in both pattern and frequency, as discussed in [30]. These advancements contribute to the development of more flexible and adaptive antenna systems that can meet diverse requirements in modern communication applications.

In [31], the authors propose a flexible antenna for multi-band applications with a total area of $25 \times 35 \times 0.254\,\mathrm{mm}^3$ and a frequency-reconfigurable method. In [32], a reversible stacked microstrip patch antenna featuring two feeds and two short pins is presented and designed for applications in terrestrial land mobile systems and satellite communications. This antenna configuration allows for flexible use in various communication scenarios by enabling adjustments in its operational modes.

Additionally, [33] discusses a reconfigurable, dual-band microstrip patch antenna with a single feed and a hexagonal slot loading. This design enhances the antenna's versatility by supporting two distinct frequency bands while maintaining a compact and efficient form factor. These innovations illustrate ongoing advancements in antenna technology aimed at improving performance and adaptability for a range of communication applications. In [34], an innovative approach to designing a frequency-reconfigurable antenna tailored for Internet of Things (IoT) applications is introduced, achieving a compact form factor measuring $40 \times 40\,\mathrm{mm}^2$. To achieve frequency reconfigurability, [35] explores the use of two U-shaped slots integrated into the ground plane of an antenna. This design modification allows for dynamic adjustment of the antenna's operating frequencies, enhancing its versatility and adaptability across various communication scenarios. By incorporating the U-shaped slots, the antenna can effectively switch between different frequency bands, thus supporting a broader range of applications. In [36], a reconfigurable dual-band antenna using four PIN diodes is presented. In [37], the authors propose a reconfigurable fractal antenna with RF MEMS switches, with dimensions of $40 \times 45\,\mathrm{mm}^2$.

A reconfigurable antenna is considered one of the most effective solutions for achieving a broad bandwidth by utilizing different ON and OFF switching conditions. Typically, this reconfigurability can be achieved using RF MEMS switches, varactor diodes, and PIN diodes to create the necessary switching states. While RF MEMS switches and varactor diodes offer advantages such as reduced insertion loss and improved Q-factor, they often come with higher costs and complexities in fabrication. In this research, we have opted for RF PIN diodes due to their affordability and numerous advantages. By employing various switching conditions with these diodes, the antenna can achieve wideband and multi-band operation while maintaining a compact package size. This approach not only enhances the antenna's versatility across different frequency bands but also ensures cost-effectiveness and ease of implementation in practical applications [38].

This paper first presents a new compact miniaturized patch antenna with new geometry and good performances like ultra-bandwidth, good gain, and radiation pattern with great adaptation. Next, it introduces a reconfigurable patch antenna with two PIN diode switching on two states (ON state and OFF state) giving us a four operations mode with different resonant frequencies and bandwidths with perfect performances. This compact antenna is well suited for diverse applications, including 5G sub-6 GHz, C-band, X-band, WLAN, WiMAX, V2X, LTE, Wi-Fi 6E, and Wi-Fi 7, making it ideal for integration into small electronic devices. Notably, this antenna covers two bands: the first one ranges from 2.9 GHz to 3.8 GHz (BP1 = 900 MHz) with resonant frequency equal to 3.29 GHz, and the second one is an ultra-large bandwidth ranging from 4.5 GHz to 11.5 GHz (BP2 = 7 GHz). It demonstrates covering a lot of bands like 5G sub-6 GHz, WIMAX, WLAN, V2X, C-band, X-band, Wi-Fi 6E, Wi-Fi 7 with three resonant frequencies: 3.29 GHz, 7.68 GHz, and 10.85 GHz. Simulation results indicate that the suggested antenna achieves good performance in terms of reflection coefficient, radiation patterns, and gain across different frequency bands. The combination of frequency adaptability and a small footprint makes the proposed antenna a promising option for a variety of uses in wireless communication. For the planning of our paper, we started by introduction. Then, we have two big sections, the first one about the moon shape antenna: in the beginning, we started by antenna design methodology, after that a parametric study, then discussion about simulated and measured results; the second section about the reconfigurable antenna.

2. MOON SHAPE ANTENNA

2.1. Antenna Design Methodology

The proposed patch antenna has been fabricated on a $22 \times 18 \times 1.6\,\mathrm{mm}^3$ ($\frac{\lambda_o}{4} \times \frac{\lambda_o}{5} \times \frac{\lambda_o}{56}$) substrate with FR-4 Epoxy material of dielectric constant $\varepsilon_r = 4.3$, $\tan\delta = 0.02$, and a height $H_S = 1.6$ mm. The patch and ground are made of copper with a thickness of 0.035 mm.

TABLE 1. Dimension values of the proposed antenna.

Parameters	W_s	L_s	Rad1	Rad2	Rad3	Rad4	Rad5	L_f
Values (mm)	18	22	6.5	4	2	1.5	1	8
Parameters	**a**	**b**	**c**	**d**	**e**	**f**	**j**	**W_f**
Values (mm)	2.8	2.1	1.6	3.2	1.6	5	6	3

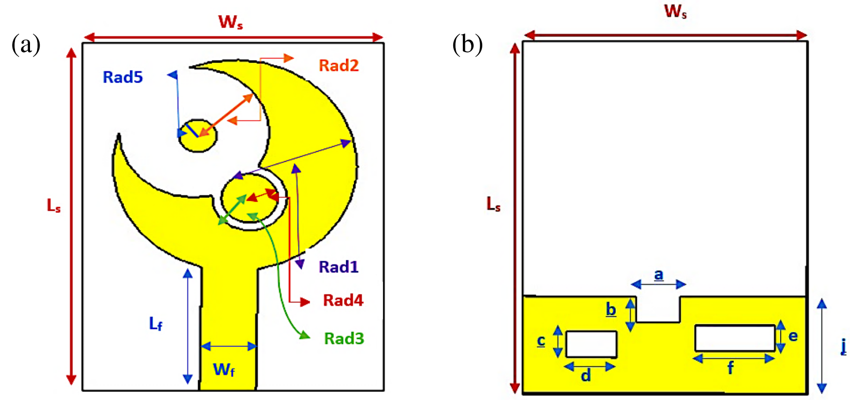

FIGURE 1. Optimized antenna: (a) Top view, (b) Back view.

The optimized parameters of this antenna are specified in Table 1. Fig. 1 shows the optimal antenna without reconfigurability in top view and back view.

The antenna receives its input from a waveguide port, with a single impedance transformation line connecting the port to the antenna. Modifying the parameters of the defected ground structure and incorporating additional slots in the patch have a discernible impact on the resonant frequency. Subsequent to simulation, the obtained results encompass metrics such as reflection coefficient, realized gain, and directivity.

The simulated S_{11} of the recommended antenna, derived from the optimized parameters, is depicted in Fig. 2.

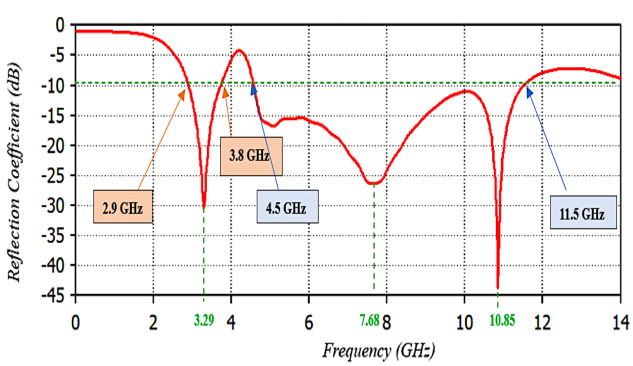

FIGURE 2. Reflection coefficient of the optimized antenna.

The following fundamental microstrip circular patch antenna design equations are used for the design [39]:

$$a = \frac{F}{\left(1+\frac{2h}{\pi\varepsilon_r F\left[ln\left(\frac{\pi F}{2h}\right)+1.7726\right]}\right)^{\frac{1}{2}}} \tag{1}$$

where:

$$F = \frac{8.791\times10^9}{f_r\varepsilon_r} \tag{2}$$

To analyze the influence of specific parameters and assess the variation's impact on the reflection coefficient, Fig. 3 illustrates the progressive steps of the antenna creation while Fig. 4 depicts the reflection coefficient in each step.

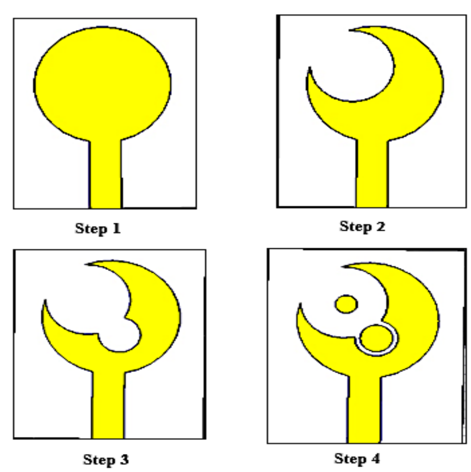

FIGURE 3. Steps for the design of patch antenna.

The process starts with an initial circular copper patch, a basic and simple design commonly found in the literature with two resonant frequencies: 3.7 GHz and 8.3 GHz. In the second step, a circular section is removed from the initial patch, transforming it into a moon shape. This simple geometric change in the patch can alter the antenna's radiating properties, resulting

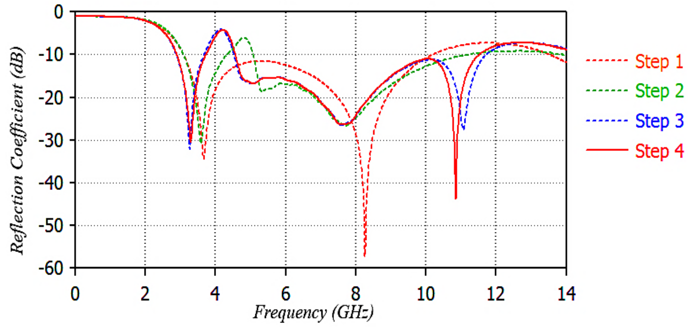

FIGURE 4. Variation of S_{11} in each step of the design.

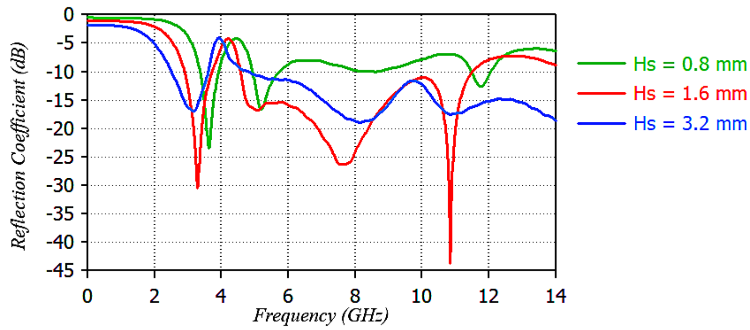

FIGURE 5. Variation of S_{11} for different thickness of substrate.

in resonant frequencies at 3.6 GHz and 7.9 GHz, with a bandwidth of 5 GHz. Next in the third step, another circular section, smaller than the first one, is removed within the crescent shape. Following this, a circular copper element, referred to as the radiating element, is added into the gap created in the previous step, which leads to three resonant frequencies: 3.296 GHz, 7.68 GHz, and 11 GHz. Finally, an additional radiating element is incorporated into the center of the gap created by the removal of the initial circular section, resulting in an improved reflection coefficient at these frequencies. Through these steps, the simple initial circular patch is turned into a complex and efficient antenna design. The removal and addition of elements are carefully applied to tune the antenna's properties and achieve the required performance.

It is evident that the frequency can be shifted by adjusting certain parameters in the antenna, such as the ground's plane dimensions and the substrate. Figs. 5 and 6 illustrate the variations in S_{11} for different substrate thicknesses and alterations in the ground plane, respectively. We observe that when $H_S = 0.8$ mm, the antenna resonates at frequencies below 3.4 GHz, 5 GHz, and 12 GHz with poor performances. Increasing the value to 3.2 mm results in the loss of resonance frequencies. Therefore, the appropriate value is $H_S = 1.6$ mm. When the ground plane is complete, the reflection coefficient is very low. However, as the ground plane becomes partial, the antenna resonates at resonant frequencies with average S_{11}. In the last step, after removing three portions of the ground, the reflection coefficient is significantly improved and becomes equal to -30 dB at 3.29 GHz, -27 dB at 7.68 GHz, and -44 dB at 10.85 GHz.

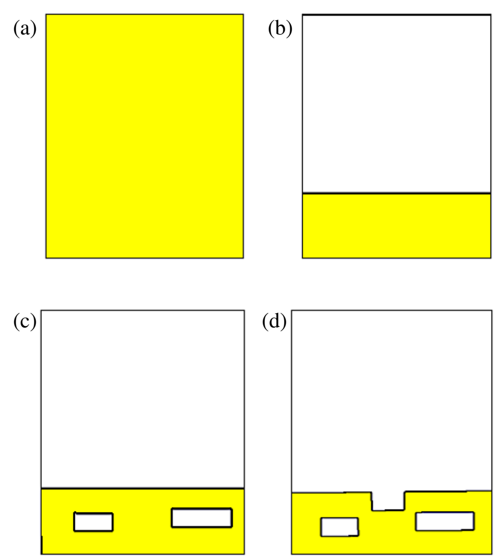

FIGURE 6. Steps for the design of the ground plane.

Figures 6 and 7 outline the design process of the antenna's ground plane and its impact on the reflection coefficient S_{11}. Fig. 6 presents the steps in the plane's design. In step 1, the ground is fully completed. In step 2, the ground is made partial, covering only a portion of the area. Step 3 introduces two slots into the partial ground plane, and finally, step 4 shows the proposed design. Fig. 7 illustrates the corresponding reflection coefficient S_{11} for each design step. When the ground plane is fully completed in step 1, the antenna resonates at approxi-

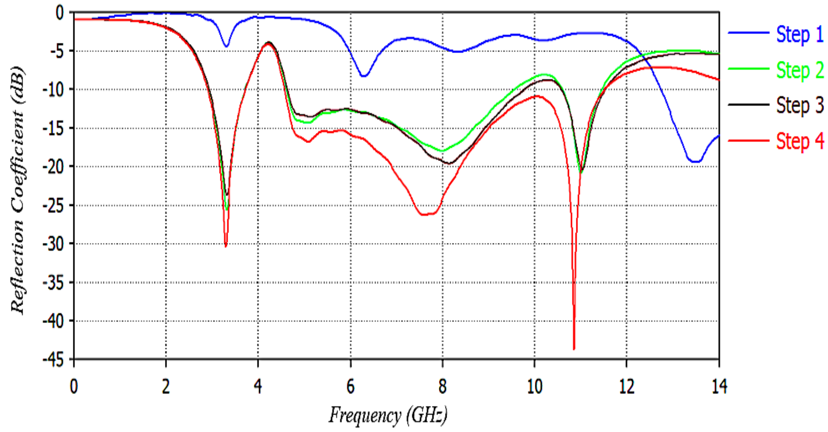

FIGURE 7. Variation of the ground plane.

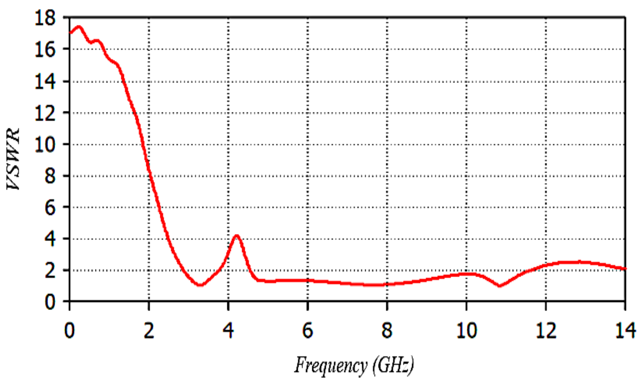

FIGURE 8. Simulated VSWR of the suggested antenna.

mately 13.5 GHz, with minimal effect at other frequencies. As the ground plane becomes partial in step 2, the resonance shifts to 11 GHz, and a new resonance appears at 3.29 GHz. The introduction of two slots in step 3 further improves the reflection coefficient. Finally, the proposed design in step 4 achieves an optimized S_{11} response, indicating enhanced performance across the frequency spectrum.

According to the literature, effective adaptation of an antenna is typically characterized by a Voltage Standing Wave Ratio (VSWR) value of less than 2 [40]. Fig. 8 illustrates that a VSWR below 2 indicates good impedance matching between the antenna and its feed network, leading to optimal performance and minimal signal reflection [41].

A VSWR value under 2 means that less than 10% of the incident power is reflected, with 90% effectively transferred to the antenna. This level of performance is excellent, indicating efficient impedance matching and minimal signal loss, thus confirming the antenna's high effectiveness in power delivery and reception, and enhancing its overall performance reliability in communication applications.

2.2. Parametric Study

In our study, we have investigated the impact of varying the length and width of the substrate on the antenna. These dimensions influence not only the resonant frequency but also the coupling between the antenna and the ground. As a result, the reflection coefficient decreases, indicating improved impedance matching. The parametric study, detailing the influence of the two substrate dimensions, is illustrated in the following figures (Fig. 9 and Fig. 1). In Fig. 9, the width of the substrate W_s was varied from 15 mm to 22 mm. We observed that the reflection coefficient improved as the width was adjusted, with an optimal value of 18 mm providing the best impedance matching across the frequency range.

Similarly, in Fig. 10, the length of the substrate L_s was varied from 20 mm to 26 mm. The results indicate that a length of 22 mm yields the optimal reflection coefficient, ensuring effective antenna performance.

Figures 11 and 12 illustrate the impact of varying the parameters Rad 4 and Rad 5 on the simulated reflection coefficients S_{11} of the antenna. In Fig. 11, it is evident that changes in Rad 4 have a limited effect on S_{11}. Rad 4 only has three viable values: increasing it beyond 1.5 mm is not practical, as the circular section would no longer be removed, while reducing it below 0.5 mm yields no meaningful results. Thus, the optimal value for Rad 4 is determined to be 1.5 mm.

In contrast, Fig. 12 indicates that altering Rad 5 has a more pronounced impact on the reflection coefficient S_{11}, with more variation observed across the different values. Among the tested values, 1 mm appears to be the optimal choice for Rad 5. Using these optimal values for Rad 4 and Rad 5 results in improved bandwidth performance.

2.3. Simulated & Measured Results and Discussion

A Ceyear vector network analyzer (model 3656D) was utilized to measure the S parameters of the printed antenna. Figs. 13 and 14 show the prototype of the proposed antenna and the corresponding measured data, respectively. The measurements reveal that the VSWR and reflection coefficient curves are generally consistent with the modeling results.

However, some discrepancies are noted, including noisy VSWR readings and slight shifts in the reflection coefficient values at the resonant frequencies. These issues are attributed to soldering problems on the feed line and ground plane, as well

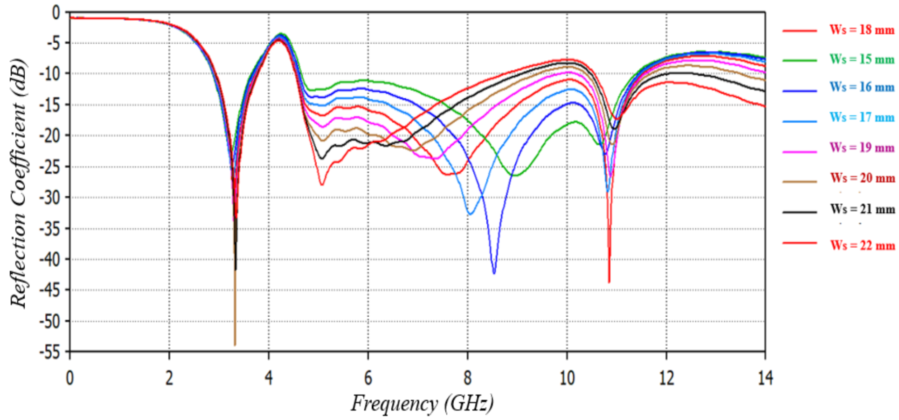

FIGURE 9. Simulated S_{11} of the antenna varies as function of W_S.

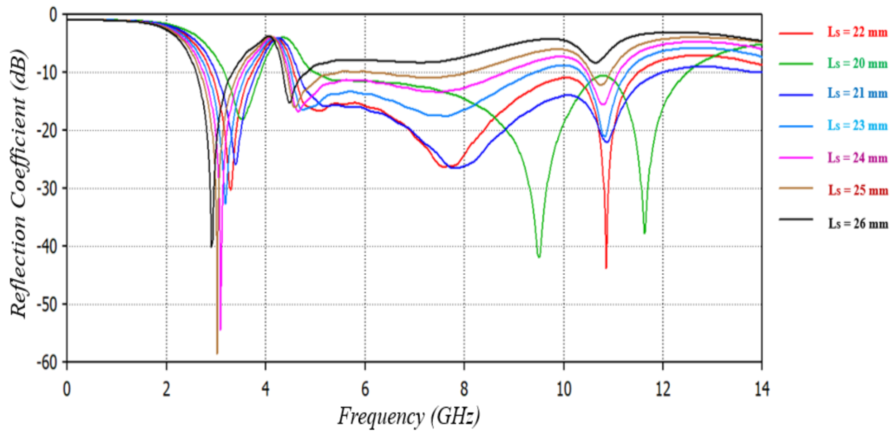

FIGURE 10. Simulated S_{11} of the antenna varies as function of L_S.

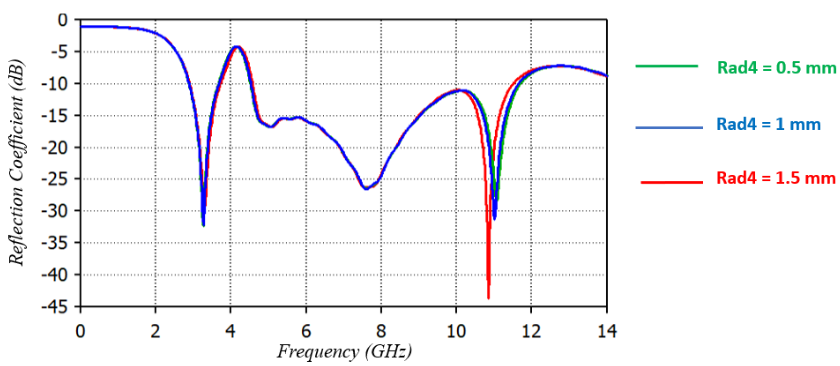

FIGURE 11. Simulated S_{11} of the antenna varies as function of Rad 4.

as interference from waves traversing the antenna's radiation field. These factors highlight the need for careful attention to soldering and potential sources of interference during the testing phase.

The surface current distribution at the three resonant frequencies is shown in Fig. 15. At 3.29 GHz, the current is primarily concentrated at the lower section of the patch antenna and within the circular element at the center. At 7.68 GHz, the current spreads slightly, with noticeable concentration at the lower part of the antenna and along the lower edge of the moon-shaped element. Finally, at 10.85 GHz, the current is concentrated in the upper part of the antenna, particularly at the extremities of the moon-shaped elements and the central circular area.

Fig. 16 illustrates the radiation patterns of the resonant frequencies (E-plane and H-plane), which are bi-directional in the E-plane and perfectly omnidirectional in the H-plane.

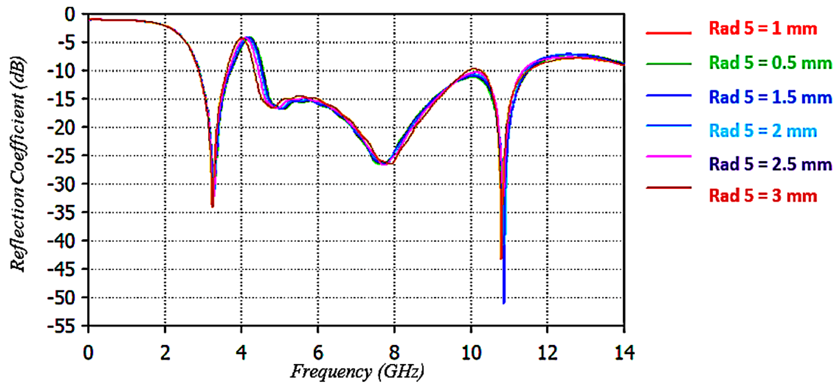

FIGURE 12. Simulated S_{11} of the antenna varies as function of Rad 5.

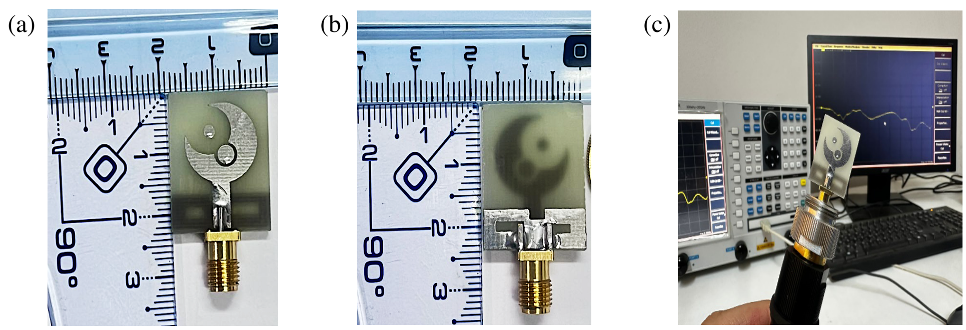

FIGURE 13. Constructed antenna prototype: (a) Top view, (b) Bottom view, and (c) The antenna with VNA.

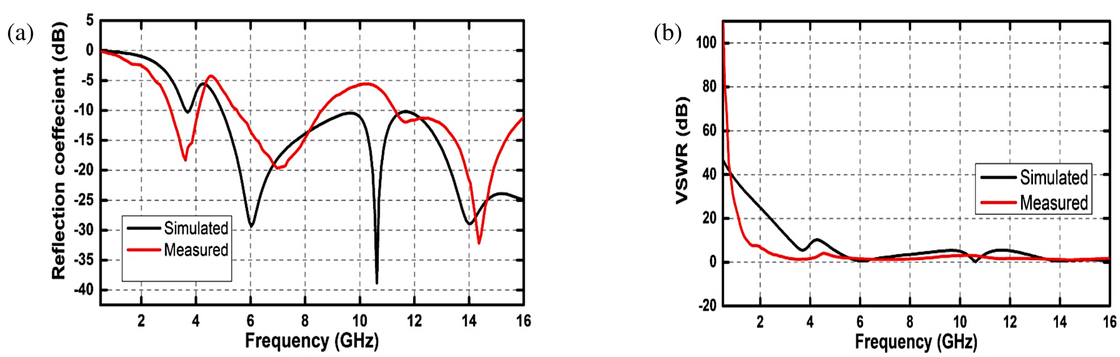

FIGURE 14. Measured and simulated results: (a) Reflection coefficient and (b) VSWR.

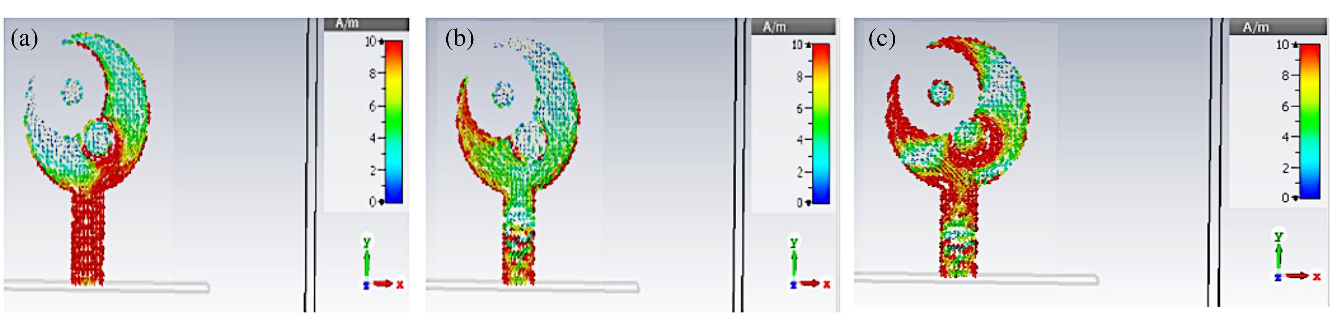

FIGURE 15. Surface current distribution at the three resonant frequencies. (a) 3.29 GHz, (b) 7.68 GHz, and (c) 10.85 GHz.

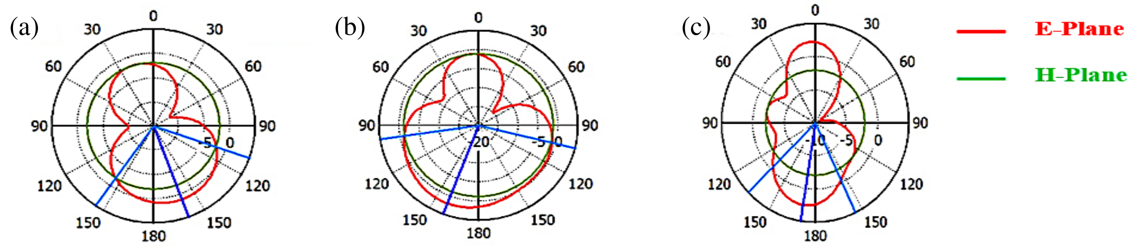

FIGURE 16. 2D radiation pattern at the three resonant frequencies. (a) 3.29 GHz, (b) 7.68 GHz, and (c) 10.85 GHz.

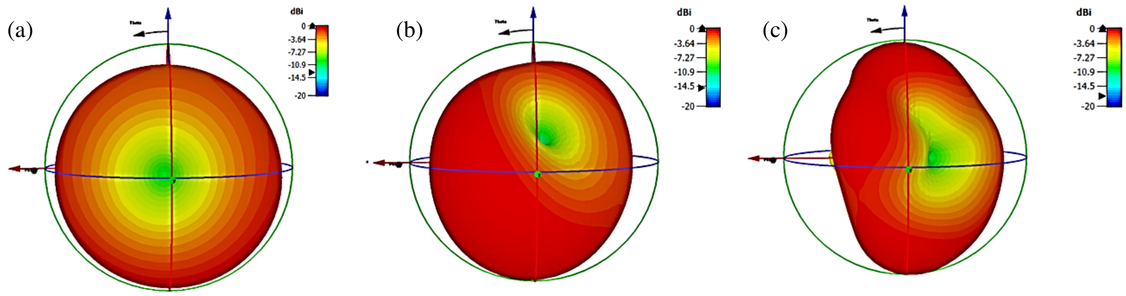

FIGURE 17. 3D radiation pattern at the three resonant frequencies. (a) 3.29 GHz, (b) 7.68 GHz, and (c) 10.85 GHz.

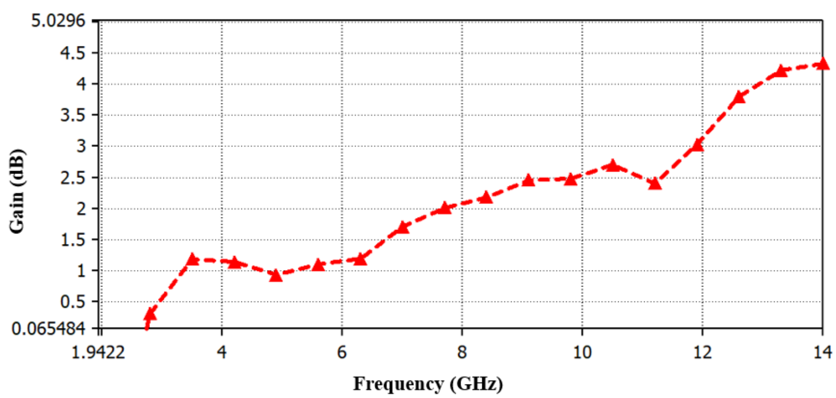

FIGURE 18. Gain vs frequency plot.

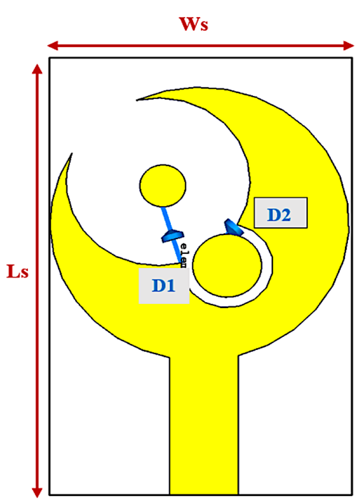

FIGURE 19. Frequency-reconfigurable antenna structure.

The realized gain of the proposed antenna at the resonant frequencies is: 1.03 dB, 2.01 dB, and 2.50 dB, respectively (Fig. 17). The directivity is: 2.91 dB at 3.296 GHz, 3.27 dB at 7.68 GHz, and 4.39 dB at 10.85 GHz, and these values indicate a stable radiation pattern, rendering the antenna suitable for various applications. Fig. 18 shows gain vs frequency plot.

3. RECONFIGURABLE ANTENNA

3.1. Antenna Design Methodology

This section details the design of the proposed reconfigurable antenna, with the front perspective illustrated in Fig. 19. To achieve frequency reconfigurability, the antenna uses PIN diodes, which are well suited for this application due to their compact size, rapid switching, and reliability. Their integration allows the antenna to dynamically adjust its operating frequencies, enhancing its versatility and performance across different communication scenarios.

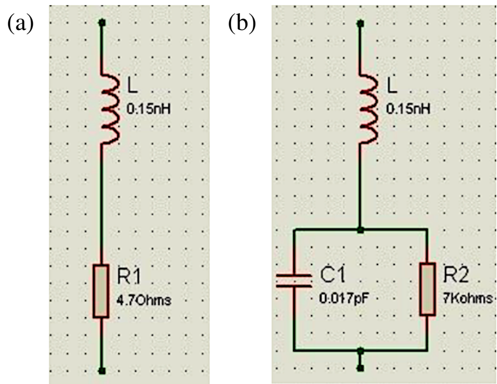

FIGURE 20. PIN diode equivalent circuit: (a) ON state, (b) OFF state.

Figure 20 depicts a simplified RLC model equivalent to the PIN diode. For simulation purposes, the PIN diode is replaced by this simplified model, obtained from the manufacturer's data sheet. The inductance L has a value of 0.15 nH in both the OFF and ON states. When the PIN diode is activated, the equivalent model can be depicted as a series combination of the 4.7 Ω resistor and L inductance. Alternatively, when the PIN diode is in the deactivated state, the equivalent model consists of two parallel elements: a 0.017 pF capacitor and a 7 kΩ resistor, which are in series with the L inductance. Table 2 summarizes the values of these passive components of the PIN diode.

TABLE 2. Values of PIN diode equivalent circuit components.

State of the diode	Components			
	L (nH)	$R1$ (Ω)	$R2$ (kΩ)	$C1$ (pF)
ON	0.15	4.7		
OFF	0.15		7	0.017

CST MWS simulation software is utilized to model the PIN diode using lumped elements, as depicted in Fig. 21. To enable frequency reconfigurability in the proposed reconfigurable antenna, two PIN diodes were employed, as shown in Fig. 21. These diodes can be in either ON or OFF state, facilitating four modes of operation, as summarized in Table 3. During simulation, the PIN diode was substituted.

In order to create a frequency-reconfigurable antenna that satisfies the needs of 5G, WLAN, WiMAX, C-band, X-band,

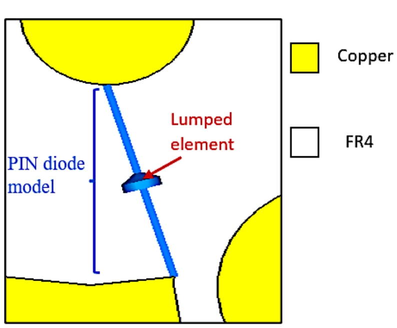

FIGURE 21. Modeling PIN diode behavior in CST MWS.

LTE, V2X, Wi-Fi 6E, and Wi-Fi 7 applications, the diode placements have been optimized.

3.2. Simulated Results and Discussion

By toggling the state of diodes D1 and D2, it is possible to either connect or disconnect the two sections of the radiating patch, resulting in a shift in operating frequencies. Fig. 22 depicts the outcomes of the S_{11} reflection coefficients for the various operating modes. The comparison of resonant frequency and bandwidth outcomes achieved for each operating mode is presented in Table 4.

In Mode 1, both D1 and D2 are turned ON. As shown in Fig. 22, the antenna in Mode 1 has resonant frequencies at 3.16 GHz and 7.84 GHz. Additionally, it has a second bandwidth that spans from 3.9 GHz to 12.8 GHz. In this mode, the antenna operates in 5G sub-6 GHz, WLAN, WiMAX, Wi-Fi 6E, Wi-Fi 7, C-band, and X-band.

In mode 2, with D1 ON and D2 OFF, the reconfigurable antenna produces three resonant frequencies at 3.27 GHz, 7.61 GHz, and 11.58 GHz. It also covers three frequency bands: 2.9 GHz to 3.63 GHz, 4.18 GHz to 10.33 GHz, and 10.55 GHz to 12.58 GHz. This makes the antenna well suited for applications in LTE, WiMAX, WLAN, as well as C-band and X-band wireless communication systems.

In Mode 3, with D1 OFF and D2 ON, the reconfigurable antenna exhibits resonant frequencies of 3.19 GHz and 7.79 GHz. It operates across two distinct frequency bands: 2.86 GHz to 3.53 GHz and 4.36 GHz to 12.4 GHz. These characteristics make the antenna highly suitable for LTE, WiMAX, WLAN, as well as C-band and X-band wireless communication systems.

Figure 22 shows the variation of simulated reflection coefficients S_{11} for the reconfigurable antenna in Mode 4. The antenna in this mode operates within two frequency bands: 2.9 GHz to 3.72 GHz and 4.56 GHz to 11.27 GHz, with resonant frequencies at 3.3 GHz, 7.57 GHz, and 10.55 GHz. This mode enables the antenna to function effectively for WLAN, WiMAX, C-band, X-band, LTE, and 5G applications.

Table 3 shows the different operating modes of the proposed reconfigurable antenna. We see nine different operational bands, which make our antenna suitable for a lot of wireless applications.

Figure 23 shows the surface current distributions at the different operating modes. When the diode in the OFF state, the current's flux is blocked, but when it is in the ON state, the current is concentrated near the diode's position.

Table 4 compares the performance of our reconfigurable antenna with that of other recently published reconfigurable antennas, focusing on the number of switches, operating bands, bandwidth, gain, and size. Notably, our proposed frequency-reconfigurable antenna operates across nine distinct bands while utilizing a minimal number of PIN diodes. This highlights the excellent performance of our compact reconfigurable antenna.

TABLE 3. Operating modes of the proposed reconfigurable antenna.

Mode	State of the diode		Resonant Frequencies (GHz)	Operational Band (GHz)	Applications
	D1	*D2*			
Mode 1	ON	ON	3.16	2.85–3.4	5G
			7.84	3.9–12.8	C-Band, X-Band, V2X, WiMAX, WLAN, Wi-Fi 6E, Wi-Fi 7
Mode 2	ON	OFF	3.27	2.9–3.63	5G
			7.61	4.18–10.33	C-Band, V2X WiMAX, WLAN, Wi-Fi 6E, Wi-Fi 7
			11.58	10.5–12.58	X-Band
Mode 3	OFF	ON	3.19	2.86–3.53	5G
			7.79	4.36–12.4	C-Band, X-Band, V2X, WiMAX, WLAN, Wi-Fi 6E, Wi-Fi 7
Mode 4	OFF	OFF	3.3	2.9–3.72	5G
			7.57	4.56–11.27	C-Band, X-Band, V2X, WiMAX, WLAN, Wi-Fi 6E, Wi-Fi 7
			10.55		

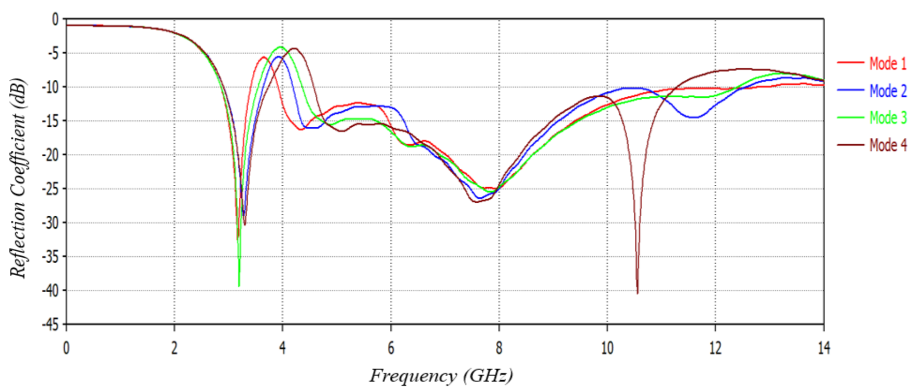

FIGURE 22. Reflection coefficient of the frequency reconfigurable antenna in all four modes.

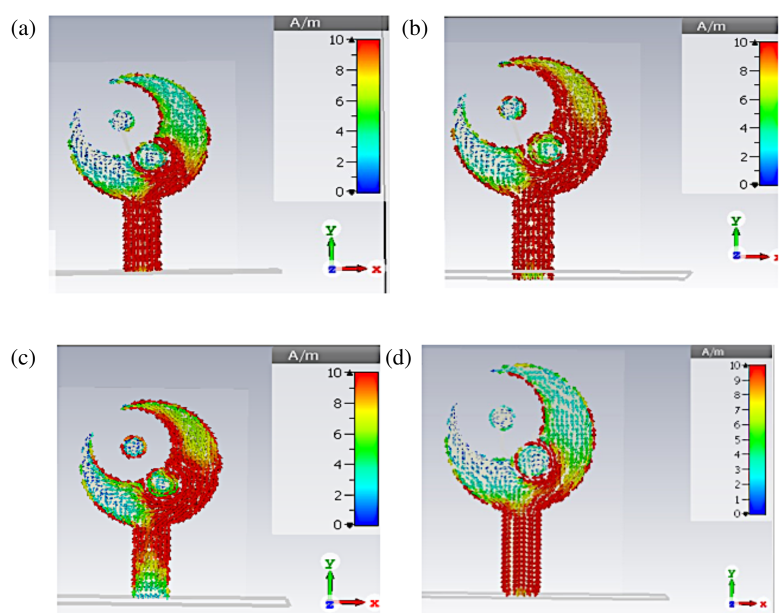

FIGURE 23. Surface current distribution at the different operating modes. (a) Mode 1 at 3.16 GHz. (b) Mode 2 at 3.27 GHz. (c) Mode 3 at 3.19 GHz. (d) Mode 4 at 3.16 GHz.

TABLE 4. Comparison with published work.

Ref	Size (mm^2)	Reconfigurability	Number of operating bands	Bandwidth (MHz)	Number of Switches	Gain (dB)
[5]	50×50	Yes	1	1500 & 1200 & 1400	4	9.1 & 6.6 & 7.4
[6]	112×52	Yes	2	1400 & 1501	18	3.8 & 8.3
[36]	40×37.2	Yes	2	500 & 630	4	0.65 & 1.92
[42]	70.11×77	No	2	50 & 25	-	5 & 4.57
[43]	32×34	No	1	500	-	3.4
[44]	20×30	No	1	690	-	2.2
[45]	75×150	No	1	200	-	5.7
[46]	45×50	Yes	1	800	2	2.2
[39]	66.4×66.4	No	1	1190	-	7.16
[47]	13×26	No	1	880	-	2.92
[48]	113×113	Yes	2	-	14	6.2 & 6.6
[49]	52×59	Yes	8	1790 & 7190	4	4.14
Proposed	18×22	Yes	9	550 & 8900 & 730 & 6150 & 2080 & 670 & 8040 & 820 & 6710	2	0.765 & 1.82 & 1.01 & 1.93 & 3.04 & 0.882 & 1.8 & 1.03 & 1.94

4. CONCLUSION

This study demonstrates the versatility of a compact reconfigurable antenna designed for a range of wireless applications. The antenna operates across nine distinct frequency bands, which are selectively activated based on different switching conditions. It boasts a radiation efficiency of 75%, and its Voltage Standing Wave Ratio (VSWR) is optimized to ideal levels. The radiation pattern of the antenna is nearly omnidirectional across all frequency ranges, ensuring broad coverage. Additionally, the simulated reflection coefficient remains within the optimal range across all frequency bands, indicating effective performance. The design of the antenna not only emphasizes compactness but also enhances bandwidth, making it suitable for various wireless communication systems. Looking ahead, future developments will include the integration of RF MEMS switches and varactor diodes to replace the current PIN diodes used for switching. A hardware model of the antenna will also be constructed to further validate its performance. Overall, the proposed frequency-reconfigurable antenna shows significant promise for improving the flexibility and efficiency of wireless communication technologies.

ACKNOWLEDGEMENT

The authors wish to extend their heartfelt appreciation to Universiti Teknikal Malaysia Melaka (UTeM) for their unwavering support and remarkable contributions. We are deeply grateful for the outstanding facilities and exceptional assistance provided, which were pivotal to the success of this research endeavor.

REFERENCES

[1] Yahya, M. S., S. Soeung, S. K. A. Rahim, U. Musa, S. S. B. Hashwan, and M. A. Haque, "Machine learning-optimized compact frequency reconfigurable antenna with RSSI enhancement for long-range applications," *IEEE Access*, Vol. 12, 10 970–10 987, 2024.

[2] Musa, U., S. M. Shah, H. A. Majid, I. A. Mahadi, K. A. R. Mohamad, M. S. Yahya, and Z. Z. Abidin, "Investigation of the nonlinearity of PIN diode on frequency reconfigurable patch antenna," *The Journal of Engineering*, Vol. 2023, No. 9, e12308, 2023.

[3] Han, L., J. Chen, G. Han, X. Chen, R. Ma, and W. Zhang, "A miniaturized reconfigurable unlicensed ultra-wideband antenna with multiple band-notch performance," *International Journal of RF and Microwave Computer Aided Engineering*, Vol. 31, No. 8, e22706, 2021.

[4] Purnamirza, T. and et al., "Return loss improvement of radial line slot array antennas on closed ring resonator structure at 28 GHz," *Przegląd Elektrotechniczny*, 65–69, 2021.

[5] Ahn, B. K., H.-W. Jo, J.-S. Yoo, J.-W. Yu, and H. L. Lee, "Pattern reconfigurable high gain spherical dielectric resonator antenna operating on higher order mode," *IEEE Antennas and Wireless Propagation Letters*, Vol. 18, No. 1, 128–132, 2019.

[6] Shereen, M. K., M. I. Khattak, and M. Al-Hasan, "A frequency and radiation pattern combo-reconfigurable novel antenna for 5G applications and beyond," *Electronics*, Vol. 9, No. 9, 1372, 2020.

[7] Boufrioua, A., "Frequency reconfigurable antenna designs using PIN diode for wireless communication applications," *Wireless Personal Communications*, Vol. 110, No. 4, 1879–1885, 2020.

[8] Bharathidevi, B. and J. Kumar, "Effect of PIN diode integration on patch antennas for frequency reconfigurable antenna applications," *Advances in Technology Innovation*, Vol. 8, No. 3, 210–218, 2023.

[9] Jin, G., C. Deng, Y. Xu, J. Yang, and S. Liao, "Differential frequency-reconfigurable antenna based on dipoles for sub-6 GHz 5G and WLAN applications," *IEEE Antennas and Wireless Propagation Letters*, Vol. 19, No. 3, 472–476, 2020.

[10] Singh, A. K., S. K. Mahto, R. Sinha, M. Alibakhshikenari, A. J. A. Al-Gburi, A. Ahmad, L. Kouhalvandi, B. S. Virdee, and M. Dalarsson, "Low-loss paper-substrate triple-band-frequency reconfigurable microstrip antenna for sub-7 GHz applications," *Sensors*, Vol. 23, No. 21, 8996, 2023.

[11] Zainarry, S. N. M., N. Nguyen-Trong, and C. Fumeaux, "A frequency-and pattern-reconfigurable two-element array antenna," *IEEE Antennas and Wireless Propagation Letters*, Vol. 17, No. 4, 617–620, 2018.

[12] Al-Gburi, A. J. A., I.-M. Ibrahim, Z. Zakaria, M. Y. Zeain, H. Alwareth, A. M. Ibrahim, and H. H. Keriee, "High Gain of UWB CPW-fed mercedes-shaped printed monopole antennas for UWB applications," *Prz. Elektrotechniczny*, Vol. 97, No. 5, 70–73, 2021.

[13] Benkhadda, O., M. Saih, A. Reha, S. Ahmad, K. Chaji, H. Singh, and A. J. A. Al-Gburi, "A miniaturized reconfigurable antenna for modern wireless applications with broadband and multi-band capabilities," *Progress In Electromagnetics Research M*, Vol. 127, 93–101, 2024.

[14] Jin, G., C. Deng, J. Yang, Y. Xu, and S. Liao, "A new differentially-fed frequency reconfigurable antenna for WLAN and sub-6 GHz 5G applications," *IEEE Access*, Vol. 7, 56 539–56 546, 2019.

[15] Awan, W. A., N. Hussain, S. A. Naqvi, A. Iqbal, R. Striker, D. Mitra, and B. D. Braaten, "A miniaturized wideband and multi-band on-demand reconfigurable antenna for compact and portable devices," *AEU — International Journal of Electronics and Communications*, Vol. 122, 153266, 2020.

[16] Lakrit, S., S. Das, A. E. Alami, D. Barad, and S. Mohapatra, "A compact UWB monopole patch antenna with reconfigurable Band-notched characteristics for Wi-MAX and WLAN applications," *AEU — International Journal of Electronics and Communications*, Vol. 105, 106–115, 2019.

[17] Khan, M. S., A. Iftikhar, A.-D. Capobianco, R. M. Shubair, and B. Ijaz, "Pattern and frequency reconfiguration of patch antenna using PIN diodes," *Microwave and Optical Technology Letters*, Vol. 59, No. 9, 2180–2185, 2017.

[18] Vanka, S. and C. Chandrasekhar, "A miniaturized-slotted planar MIMO antenna with switchable configuration for dual-/triple-band notches," *AIP Advances*, Vol. 14, No. 2, 025039, 2024.

[19] Gupta, S. K. and A. Bage, "A compact dual-band frequency reconfigurable MIMO antenna for 5G/WLAN/Wi-MAX applications," *Thailand-Japan MicroWave Workshop and Asian Wireless Power Transfer Workshop 2023 (TJMW&AWPT 2023)*, 2023.

[20] El Aoud, S. E., H. Abbaoui, S. Attioui, S. Ibnyaich, A. Ghammaz, A. Zeroual, and H. Belahrach, "Design of ultra wideband triangular shaped patch antenna for 39 GHz millimiter-wave applications," in *2024 International Conference on Global Aeronautical Engineering and Satellite Technology (GAST)*, 1–5, Marrakesh, Morocco, Apr. 2024.

[21] Zhao, K., S. Zhang, Z. Ho, O. Zander, T. Bolin, Z. Ying, and G. F. Pedersen, "Spherical coverage characterization of 5G millimeter wave user equipment with 3GPP specifications," *IEEE Access*, Vol. 7, 4442–4452, 2018.

[22] Al Ahmad, M., S. Kabeer, A. A. Sanad, and L. J. A. Olule, "Compact single-varactor diode frequency-reconfigurable microstrip patch antenna," *IET Microwaves, Antennas & Propagation*, Vol. 15, No. 9, 1100–1107, 2021.

[23] Gençoğlan, D. N., S. Çolak, and M. Palandöken, "Spiral-resonator-based frequency reconfigurable antenna design for sub-6 GHz applications," *Applied Sciences*, Vol. 13, No. 15, 8719, 2023.

[24] Kareem, Q. H. and R. A. Shihab, "Reconfigurable compact quad-port MIMO antennas for sub-6 GHz applications," *Journal of Al-farabi for Engineering Sciences*, Vol. 2, No. 1, 2023.

[25] Wappi, F. D., B. Mnasri, A. Ghayekhloo, L. Talbi, and H. Boutayeb, "Miniaturized compact reconfigurable half-mode SIW phase shifter with PIN diodes," *Technologies*, Vol. 11, No. 3, 63, 2023.

[26] Yasin, F. N. M., N. A. Shairi, A. Othman, H. A. Majid, Z. Zakaria, I. M. Ibrahim, and M. H. Jamaluddin, "High isolation of SPDT PIN diode switch using switchable dumbbell-shaped DGS in millimeter wave 28 GHz band," *Bulletin of Electrical Engineering and Informatics*, Vol. 12, No. 6, 3509–3516, 2023.

[27] El Yassini, A., M. A. Jallal, S. Ibnyaich, A. Zeroual, and S. Chabaa, "A miniaturized CPW-fed reconfigurable antenna with a single-dual band and an asymmetric ground plane for switchable band wireless applications," *International Information and Engineering Technology Association*, Vol. 37, No. 4, 633–638, 2020.

[28] Tiwari, A., D. Yadav, P. Sharma, and M. V. Yadav, "Design of wide notched-band circular monopole ultra-wideband reconfigurable antenna using PIN diodes switches," *Progress In Electromagnetics Research C*, Vol. 139, 107–118, 2024.

[29] Piazza, D., N. J. Kirsch, A. Forenza, R. W. Heath, and K. R. Dandekar, "Design and evaluation of a reconfigurable antenna array for MIMO systems," *IEEE Transactions on Antennas and Propagation*, Vol. 56, No. 3, 869–881, 2008.

[30] Nikolaou, S., R. Bairavasubramanian, C. Lugo, I. Carrasquillo, D. C. Thompson, G. E. Ponchak, J. Papapolymerou, and M. M. Tentzeris, "Pattern and frequency reconfigurable annular slot antenna using PIN diodes," *IEEE Transactions on Antennas and Propagation*, Vol. 54, No. 2, 439–448, 2006.

[31] Thanki, P. and F. Raval, "I-shaped frequency and pattern reconfigurable antenna for WiMAX and WLAN applications," *Progress In Electromagnetics Research Letters*, Vol. 97, 149–156, 2021.

[32] Ali, M., A. T. M. Sayem, and V. K. Kunda, "A reconfigurable stacked microstrip patch antenna for satellite and terrestrial links," *IEEE Transactions on Vehicular Technology*, Vol. 56, No. 2, 426–435, 2007.

[33] Shynu, S. V., G. Augustin, C. K. Aanandan, P. Mohanan, and K. Vasudevan, "A reconfigurable dual-frequency slot-loaded microstrip antenna controlled by pin diodes," *Microwave and Optical Technology Letters*, Vol. 44, No. 4, 374–376, 2005.

[34] Riaz, S., M. Khan, U. Javed, and X. Zhao, "A miniaturized frequency reconfigurable patch antenna for IoT applications," *Wireless Personal Communications*, Vol. 123, 1871–1881, 2022.

[35] Mirzamohammadi, F., J. Nourinia, and C. Ghobadi, "A novel dual-wideband monopole-like microstrip antenna with controllable frequency response," *IEEE Antennas and Wireless Propagation Letters*, Vol. 11, 289–292, 2012.

[36] Kumar, P., S. Dwari, R. K. Saini, and M. K. Mandal, "Dual-band dual-sense polarization reconfigurable circularly polarized antenna," *IEEE Antennas and Wireless Propagation Letters*, Vol. 18, No. 1, 64–68, 2019.

[37] Nafde, Y. and R. Pande, "Design and analysis of resistive series RF MEMS switches based fractal U-slot reconfigurable antenna," *Wireless Personal Communications*, Vol. 97, 2871–2886, 2017.

[38] Sravani, K. G., D. Prathyusha, G. R. K. Prasad, C. G. Chand, P. A. Kumar, K. Guha, and K. S. Rao, "Design of reconfigurable antenna by capacitive type RF MEMS switch for 5G applications," *Microsystem Technologies*, Vol. 28, No. 3, 845–853, 2022.

[39] Varshney, A., N. Cholake, and V. Sharma, "Low-cost ELC-UWB fan-shaped antenna using parasitic SRR triplet for ISM band and PCS applications," *International Journal of Electronics Letters*, Vol. 10, No. 4, 391–402, 2022.

[40] El Aoud, S. E., H. Abbaoui, L. Aguni, Z. E. Ouadi, S. Ibnyaich, A. Ghammaz, A. Zeroual, and H. Belahrach, "Design, optimization and prediction of the performances for a multi-band patch antenna using artificial neural network (ANN)," in *International Conference on Advanced Technologies for Humanity*, 55–64, 2022.

[41] Balanis, C. A., *Antenna Theory: Analysis and Design*, John Wiley & Sons, 2016.

[42] Sree, M. F. A., M. H. A. Elazeem, and W. Swelam, "Dual band patch antenna based on letter slotted DGS for 5G Sub-6 GHz application," in *Journal of Physics: Conference Series*, Vol. 2128, No. 1, 012008, 2021.

[43] Agarwal, S. and M. P. Gupta, "Sub-6 GHz novel C-shaped antenna for 5G application," in *2022 IEEE Microwaves, Antennas, and Propagation Conference (MAPCON)*, 729–732, Bangalore, India, Dec. 2022.

[44] Kulkarni, N., R. M. Linus, and N. B. Bahadure, "A small wideband inverted L-shaped flexible antenna for sub-6 GHz 5G applications," *AEU — International Journal of Electronics and Communications*, Vol. 159, 154479, 2023.

[45] Moses, A. T. Z. and N. Moses, "Compact self decoupled MIMO antenna pairs covering 3.4-3.6 GHz band for 5G handheld device applications," *AEU — International Journal of Electronics and Communications*, Vol. 141, 153971, 2021.

[46] Ghaffar, A., X. J. Li, W. A. Awan, A. H. Naqvi, N. Hussain, M. Alibakhshikenari, and E. Limiti, "A flexible and pattern reconfigurable antenna with small dimensions and simple layout for wireless communication systems operating over 1.65-2.51 GHz," *Electronics*, Vol. 10, No. 5, 601, 2021.

[47] Varshney, A., V. Sharma, T. M. Neebha, and R. Kumar, "A compact low-cost impedance transformer-fed wideband monopole antenna for Wi-MAX N78-band and wireless applications," in *Printed Antennas*, 315–328, 1st ed., CRC Press, 2022.

[48] Ismail, M. F., M. K. A. Rahim, M. R. Hamid, H. A. Majid, A. H. Omar, L. O. Nur, and B. S. Nugroho, "Dual-band pattern reconfigurable antenna using electromagnetic band-gap structure," *AEU — International Journal of Electronics and Communications*, Vol. 130, 153571, 2021.

[49] Varshney, A., T. M. Neebha, V. Sharma, J. G. Jency, and A. D. Andrushia, "Dodecagon-shaped frequency reconfigurable antenna practically loaded with 3-delta structures for ISM band and wireless applications," *IETE Journal of Research*, Vol. 69, No. 11, 7747–7759, 2023.